

## CO<sub>2</sub> and climate change

Noor van Andel, [noor@xs4all.nl](mailto:noor@xs4all.nl), 14-02-2011.

### Summary

The tropical Pacific sea surface temperature anomalies are closely congruent to global temperature anomalies over more than a century. When we understand the cooling mechanism over the tropical Pacific, and especially its CO<sub>2</sub> dependency, we can draw conclusions for the global CO<sub>2</sub> climate sensitivity. The cooling of the tropics, or trade wind belt, is by deep convection, i.e. by a few thousand concentrated tropical thunderstorms that carry the latent heat swept up by the trade winds all the way on to the tropopause. The atmosphere is completely IR transparent at this height; heat on this height is radiated unhindered to space. The physics of deep convection have been formulated since 1958 and are based on sound thermodynamics and measurements on location.

The trends of the temperature in the high atmosphere in the last half century are very negative, on and above this height where the deep convection reaches. Cloud tops radiate much more intensely than the thin air on this height. This is the cause behind the cooling, as much as the CO<sub>2</sub> increase is. This cooling trend increases the effective environmental lapse rate and so reinforces the strength of deep convection. This means that in this respect, more CO<sub>2</sub> has a cooling effect rather than a warming effect.

This cooling trend is quite in discrepancy with the “greenhouse-gas-induced-global-warming” theory, but quite in accord with increasing deep convection. Many publications try to adjust these temperature measurements to bring them more in line with the climate models. These adjustments are an order of magnitude larger than the inaccuracy of the instruments, and lead to unphysical conditions and processes. No literature is to be found that treats adjustment of the climate models to bring them in line with the measurements, however. The response of the upper atmosphere temperature on volcanic eruptions also fits in the deep convection theory, but not in the mainstream theory. Two other parameters are candidates for the cause of climate change:

**1] ENSO or El Niño Southern Oscillation.** The large change in the cold water upwelling along the Pacific coast of South America correlates very well to short term climate change.

**2] Change in the intensity, during Forbush events, of hard and deeply penetrating Galactic Cosmic Radiation [GCR] influences in a matter of days the cloud water content, the liquid water cloud fraction and the low IR-detected clouds.** The 11 year average of northern hemispheric marine and land temperatures correlates much stronger with solar cycle length and the 11 year average of cosmic ray flux between 1937–1994 than with CO<sub>2</sub> levels in that period. The global average monthly mean anomalies of low IR cloud cover during the solar cycle 1982-1993 correlate well with the variations of GCR fluxes as measured by the Climax neutron monitor. Comparison of the low-pass filtered <sup>10</sup>Be data from the Dye3 Greenland ice core correlate well with the temperature record from central England, the oldest we have. The coincidence between wheat price bursts in medieval England (1259-1702) and intervals between minima of solar cycles (1700-2000) and the existence of 100% sign correlation between high wheat prices and states of minimal solar activity established on the basis of <sup>10</sup>Be data for Greenland ice cores for the period 1600-1700 prove the influence of GCR on climate. The timing of glacial Termination II, 130 ky ago, has been a problem for many years because it does not fit with the Milanković timing and not with the Specmap timing. But it does fit with the decreasing GCR rate as documented by <sup>10</sup>Be deposits and <sup>14</sup>C levels.

### Conclusion

Climate changes are only marginally caused by greenhouse gases. The main heat transfer process is convection, strongly increasing with sea surface temperature. Climate changes are caused by changing sea currents, and in the long run by Galactic Cosmic Radiation variations.

## Introduction

The main stream [IPCC quoted] literature on global warming is more concentrated on climate models than on interpretation of measurements. These climate models are very complex and therefore inaccessible. Can we, starting from generally accepted measurements of atmospheric quantities and generally accepted meteorological-thermodynamic relations, arrive at an alternative method to evaluate the influence of increased CO<sub>2</sub> on our climate, without using complicated numerical methods, but only clear closed mathematical derivations?

The first challenge is to simplify the climate relations. This is possible by realizing that the tropical Pacific Sea Surface Temperature [SST] varies over time such that its anomalies, deviations from the long-time mean, are a very precise indication of the anomalies in the global temperature. This is no wonder. More than half of the absorbed solar energy is absorbed in the tropics, and the Pacific is no different from the Indian and Atlantic Oceans, nor from the very wet rain forests in South America and Africa. There are no climate fronts, no cyclones or anticyclones, no depressions. The discharge of solar energy is mainly by deep convection, that is cumulonimbus clouds that reach all the way to the tropopause where the heat is convected to, radiated vertically and advected horizontally away in the so-called Hadley hydrological cycle, until the air is cold enough to subside in the desert belt. A good estimate can be given of the SST-dependence of this deep convection. Of course, the second way of cooling is radiation through the infrared window, the CO<sub>2</sub> dependency of which is well known. In this way we arrive to a “climate sensitivity” to a doubling of CO<sub>2</sub> in an alternative way, without using climate models with their inherent parametrisations.

## Tropical Pacific SST- and global temperature anomalies

Data from KNMI climate explorer show that the tropical Pacific drives the world's climate and Sea Surface Temperatures [SST] anomalies there closely match the anomalies of the global temperature:

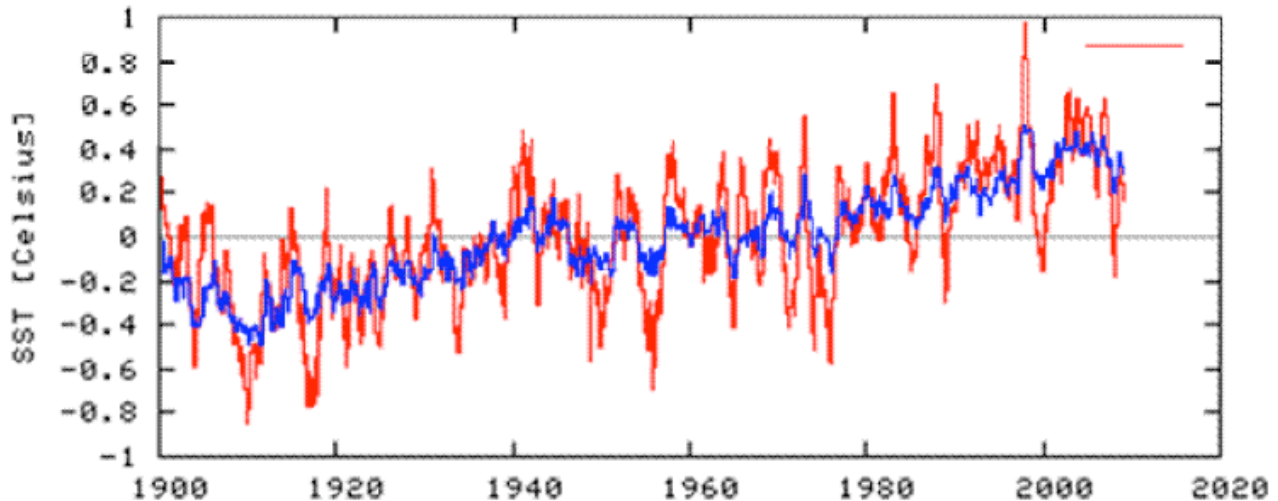


Figure 1. Red: SST anomalies Pacific 20°N-20°S; blue: global temperature anomaly.

We see in figure 1 that the noise amplitude in the Pacific SST is larger, but that it faithfully indicates global values. When we understand the heat transfer in the tropical Pacific, we can extrapolate to global values. The same is true for the climate sensitivity due to CO<sub>2</sub> increase. This makes our physical treatment much simpler. We do not need complicated climate models. We can treat the Pacific cooling mechanism with closed algebraic formulas from classic meteorology and compare the results directly with measurements.

## Mechanism of tropical Pacific cooling.

The cooling of the Pacific takes place in the Hadley cycle. Trade winds carry heat and moisture from the sea to the Intertropical Convergence Zone [ITCZ], where a series of rainstorms or deep convection towers convert this heat, mostly latent heat, to expansion until the tropopause is reached. The deep convection towers have dimensions large enough that mixing between convection chimney and environment is small. All potential height, stored in sensible & latent heat, is converted into real convection height. The tropopause height is the same as that what follows from temperature & humidity at sea level. There is no radiative heat transfer from SST to atmosphere. There is however a direct transfer from SST to space via the Infrared Window, that is the collection of all wavelengths where nor water, nor CO<sub>2</sub> have molecular absorption. There is also upgoing IR radiation from the atmosphere itself, fed by heat deposited there by absorption of visible radiation. The last two are influenced by the CO<sub>2</sub> level, but the deep convection is not, as we will show. Deep convection transports heat from the surface to the tropopause at the location of rainstorms, especially at the ITCZ. A few thousand tropical thunderstorms are enough to get rid of all the heat that is taken by evaporation from the sea surface in the trade wind zone, from 20° N to 20° S. [Riehl, H.; Malkus, J.S. (1958). "On the heat balance in the equatorial trough zone". *Geophysica* **6**: 503–538]. It is straightforward to quantify this deep convection. We have no need of climate models, but use instead straightforward physics, since long part of classical meteorology:

[http://en.wikipedia.org/wiki/Equivalent\\_potential\\_temperature](http://en.wikipedia.org/wiki/Equivalent_potential_temperature):

$$\theta_e = T_e \left( \frac{p_0}{p} \right)^{\frac{R_d}{c_p}} \approx \left( T + \frac{L_v}{c_p} r \right) \left( \frac{p_0}{p} \right)^{\frac{R_d}{c_p}}$$

wherein  $\theta_e$  is the equivalent potential temperature,  $T_e$  the equivalent temperature,  $T$  the SST,  $L_v$  the latent heat of water,  $C_p$  the heat capacity of air at constant pressure,  $L_v/C_p$  is 2500 K,  $R_d$  the gas constant,  $p_0$  and  $r$  the pressure and the specific humidity at sea level,  $p$  the air pressure.

As long as  $\theta_e$  in the convection column is larger than the  $\theta_e$  in the environment buoyancy is positive and convection continues. If we neglect the very low humidity at maximum convective height,  $\theta_e = T - ELR * h$  outside the column. If the deep convection tower diameter is large enough and mixing at the rising column boundary can be neglected, all heat collected at the bottom of the cloud will be converted to expansion and thus to upward movement and  $\theta_e$  inside the cloud is conserved.

What is the maximum convective height of a thunderstorm?

I start with a diagram which is in common use by meteorologists, see for a good explanation of theory and practice <http://www.downunderchase.com/storminfo/stormguide/index.html> .

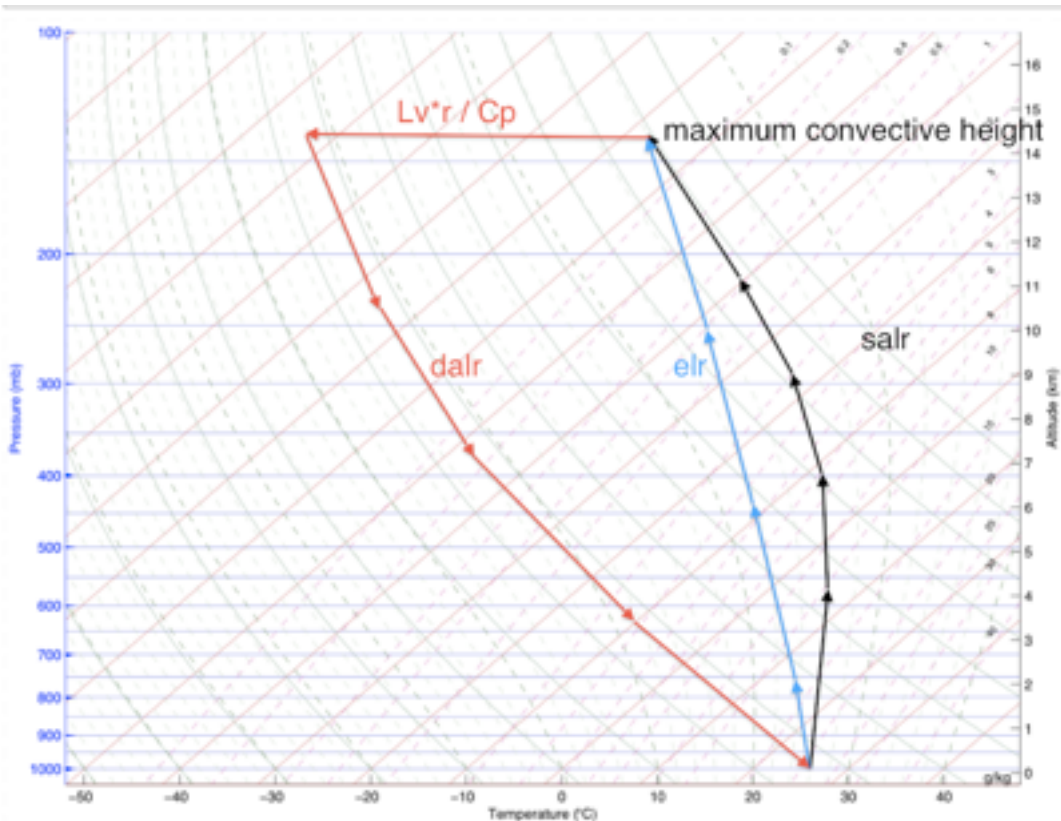


Figure 2 In this color skew-T log-p diagram, red lines are isotherms, solid green lines are lines of equal potential temperature, or dry adiabatic lapse rates [DALR], dashed green lines are lines of equal *equivalent* potential temperature  $\theta_e$  or saturated adiabatic lapse rates [SALR], all derived from the scale in °C when crossing the 1000 hPa line just above the bottom of the graph. The blue lines are isobars with the scale at the left side, and the dashed purple lines give the saturated humidity mixing ratio in g/kg, scale in the graph at the right. The right edge gives the altitude in km. For a SST of 27 °C and a specific humidity of 20 g/kg, I drew also the environmental lapse rate [ELR], that is the **measured** local lapse rate, 6.5 K/km.

For these lapse rates, see [http://en.wikipedia.org/wiki/lapse\\_rate](http://en.wikipedia.org/wiki/lapse_rate),

Let us follow an air parcel from the sea surface, 27°C warm and 20 g/kg moist. For simplicity, we neglect the height of the Lower Condensing level. The parcel rises along the SALR, the saturated Adiabatic Lapse rate, condensing and precipitating water in its rise, keeping its  $\theta_e$  constant in a thunderstorm large enough that peripheral mixing is too small to count. It will rise until the environmental  $\theta_e$ , determined by altitude and ELR, becomes as high as the  $\theta_e$  inside the cloud. That is at 140 mB or 15 km altitude, the maximum convective height  $h_{max}$ . The air is now very dry, 0.05 g/kg, so it can only descend along the dry adiabatic lapse rate DALR, but then it should get rid of its heat and cool theoretically from its -68 °C to -104 °C to reach the corresponding DALR to its origin at 28°C. This temperature distance is just the difference between  $T_e$  and  $T$  at the surface, or  $L_r/C_p$ . Of course, it descends along the DALR belonging to the temperature of the cloud top, giving a theoretical surface temperature of 90°C, so not all but most of the radiation has to be done with in the high troposphere.

We can simplify the expression for  $h_{max}$  and even can it make explicit, with thanks to W. C. Gilbert and J.W. Reynen:  $[DALR - ELR] * h_{max} = [T_e - T] = L_r/C_p$  or  $h_{max} = L_r/C_p / [DALR - ELR] = r \cdot 2500 / [9.8 - 6.5]$  km. At  $r = 20 \times 10^{-3}$  we get 15 km. We see that it is not the SST that is the principal variable, but  $r$ , or the water mass mixing rate or specific humidity, that of course is dependent on SST and the relative humidity. We see also that it is the latent heat that is delivered high up in the troposphere. The sensible heat is returned along the DALR after descent.

**maximum convective height as function of environmental lapse rate and sea level specific humidity.**

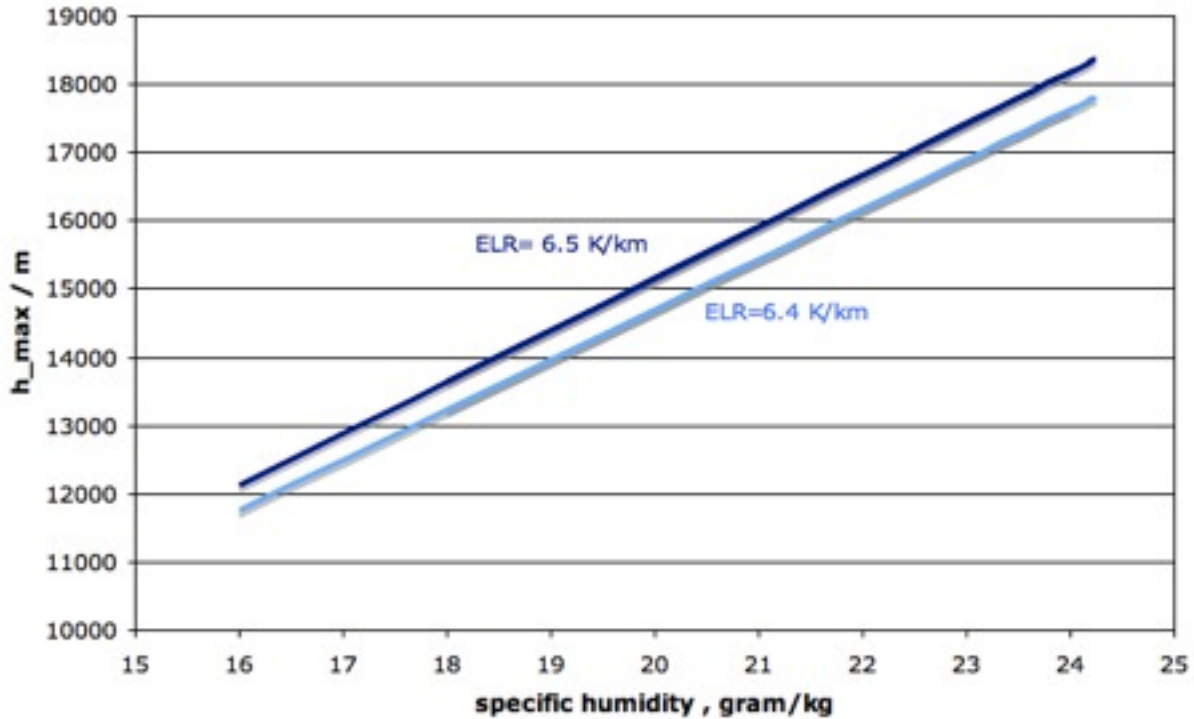


Figure 3 Maximum height of a tropical thunderstorm cloud as function of the sea level specific humidity and the environmental lapse rate.

**SST dependence of deep convective cooling**

We should now establish the dependence of the convective cooling as function of the SST. We have seen that this comes down to estimate the dependence of evaporative cooling at the sea surface as a function of SST, or the mass of water that is evaporated.

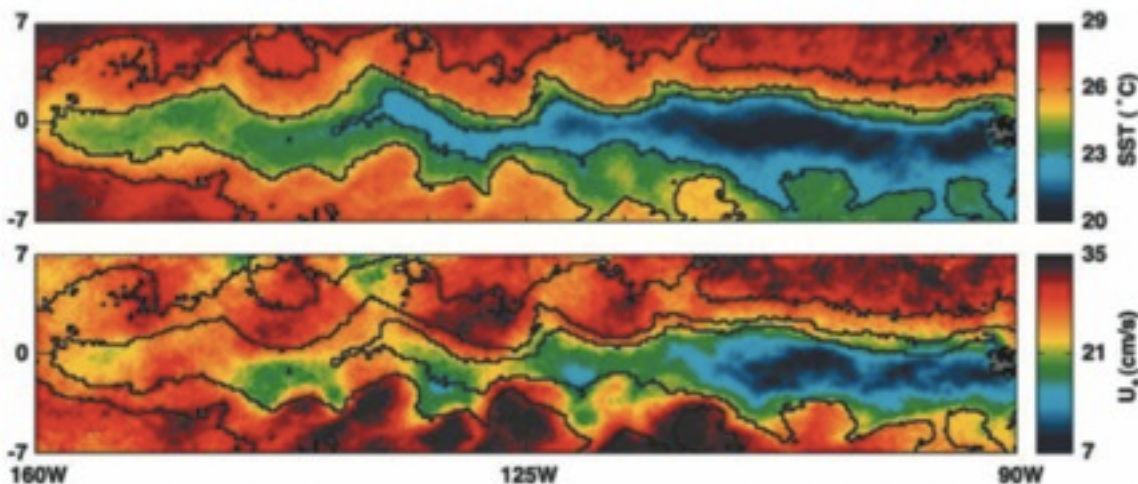


Figure 4 SST and surface wind in the vicinity of the eastern Pacific equatorial cold tongue during the first week in October 1998. The surface wind is given in terms of the friction velocity  $U_*$ . The black contour lines show the isotherms for 230, 250 and 270 C derived from the SST image. These contour lines are superimposed on the  $U$  image to highlight its correlation with SST.

Over warm water turbulent mixing increases the exchange of momentum from winds aloft to the surface. As a result, higher surface winds are associated with warmer water. Fig. 4 shows the wind shear  $U^*$  at 20 °C SST is 7 cm/s and at 29 °C SST 35 cm/s. Now  $U^*$  is proportional to  $U_{10}^2$ , so that is a factor of 2.23 in  $U_{10}$  with 9 °C SST or a factor 1.094 in  $U_{10}$  per °C SST. The evaporation rate [latent heat flow] has been measured as a function of wind speed and water surface temperature in the Lake Hefner Study, 1952. When we take their formula we arrive at 109.6 W/m<sup>2</sup> for 23 °C and 4 m/s, about the typical wind speed over the tropical Pacific. Mass transfer and latent heat flux are proportional to wind speed. This means for 24°C, 120 W/m<sup>2</sup>, for 25 °C 131 W/m<sup>2</sup>, for 26 °C, 143 W/m<sup>2</sup>, for 26°C , 156 W/m<sup>2</sup> , for 27 °C, 172 W/m<sup>2</sup>, for 28 °C, 188 W/m<sup>2</sup>., for 29°C, 205 W/m<sup>2</sup> , for 30°C, 225 W/m<sup>2</sup>. This means in the relevant SST region that **20 W/m<sup>2</sup>** is necessary for the increase of SST with 1°C.

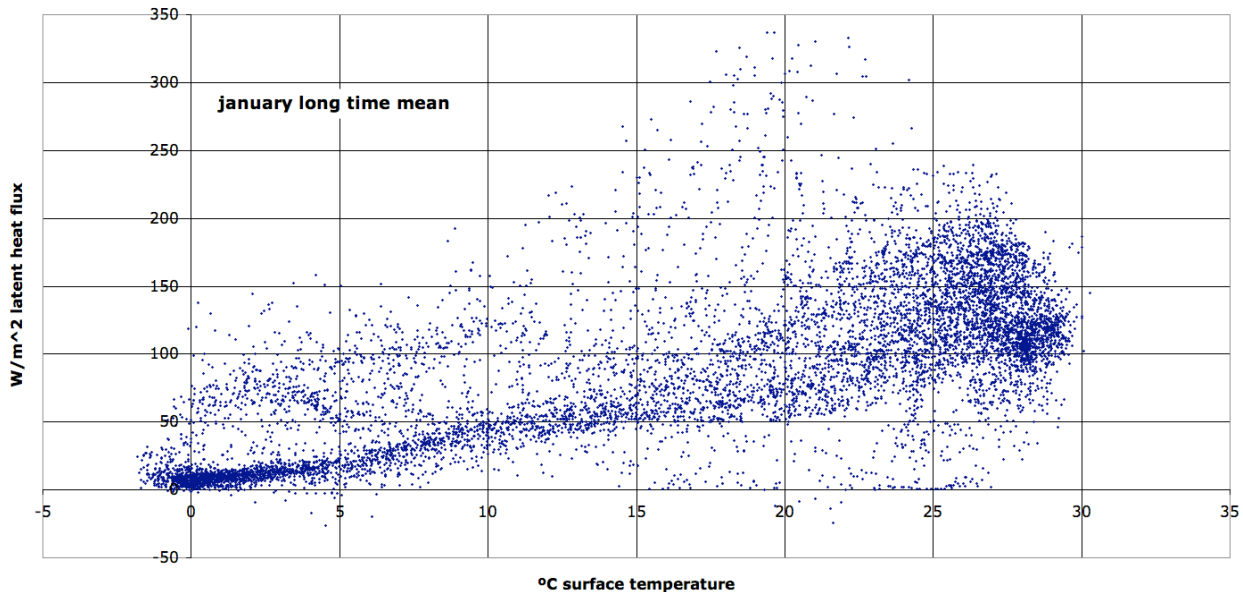


Figure 5. NCEP reanalysis scatter plot of latent heat flux and sea surface temperature.

Fig. 5 shows a trend in the relevant SST region of about **20 W/m<sup>2</sup>K**, from 170 W/m<sup>2</sup> at 25°C to 210 W/m<sup>2</sup> at 27°C. The points above 150 W/m<sup>2</sup> and 25 °C are above tropical seas.

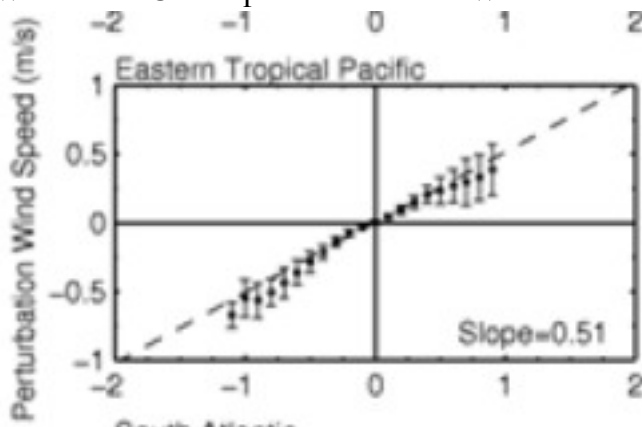


Figure 6. Regression of wind speed versus SST over the Eastern Tropical Pacific.

Fig.6 gives a SST dependency of wind 0.51 m/s per °C SST, in this case 12.7 % increase of mass or heat transfer per °C SST, or 24 W/m<sup>2</sup>, a little more than in the preceding two independent cases. We conclude that for 1 °C SST increase a **20 W/m<sup>2</sup>** extra heat flux to the sea surface is needed.

## radiation cooling of the sea surface

The other mechanism is the infrared radiation from the sea surface directly to space through the infrared window and from the troposphere itself. Miskolczi calculated this effect in *Energy & Environment* · Vol. 21, No. 4, 2010, table 3 on p. 257. For a doubling of CO<sub>2</sub> we see  $[\Delta\text{OLR}/\Delta c]$  a 3.7 W/m<sup>2</sup> decrease in OLR, that must be compensated by an increase in the deep convective heat transfer and / or an increase in SST. This 3.7 W/m<sup>2</sup> "forcing" is a generally accepted number, also by IPCC-quoted authors. Miskolczi gives the IR optical depth as function of altitude as follows: INTERNATIONAL CONFERENCE ON GLOBAL WARMING, New York, March 2-4, 2008

optical depth

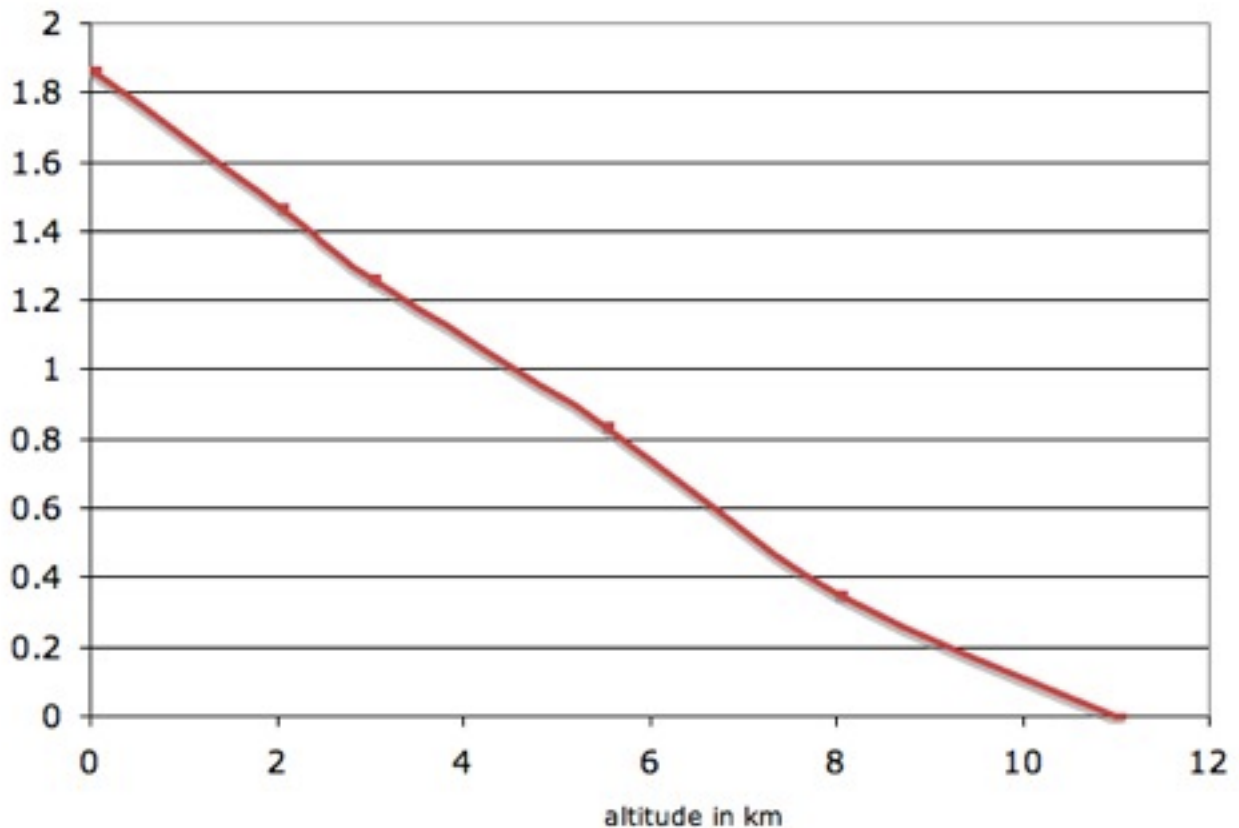


Figure 7. Infrared optical depth, or  $\ln[\text{IR absorption}]$  as a function of altitude in km.

Fig. 7 shows that at above 11 km the global average atmosphere is essentially transparent in the infrared region. The optical depth is nearly a linear function of height because the density of IR active gases decreases exponentially with height. We can conclude that for the relevant region, around 20 g/kg specific humidity, or 15 km convective cloud top, the atmosphere is transparent. The influence of H<sub>2</sub>O or CO<sub>2</sub> on outgoing radiation is zero at this altitude.

A couple of schematic drawings taken from <http://www-das.uwyo.edu/~geerts/cwx/notes/chap01/tropo.html> might illustrate the deep convective cooling mechanism.

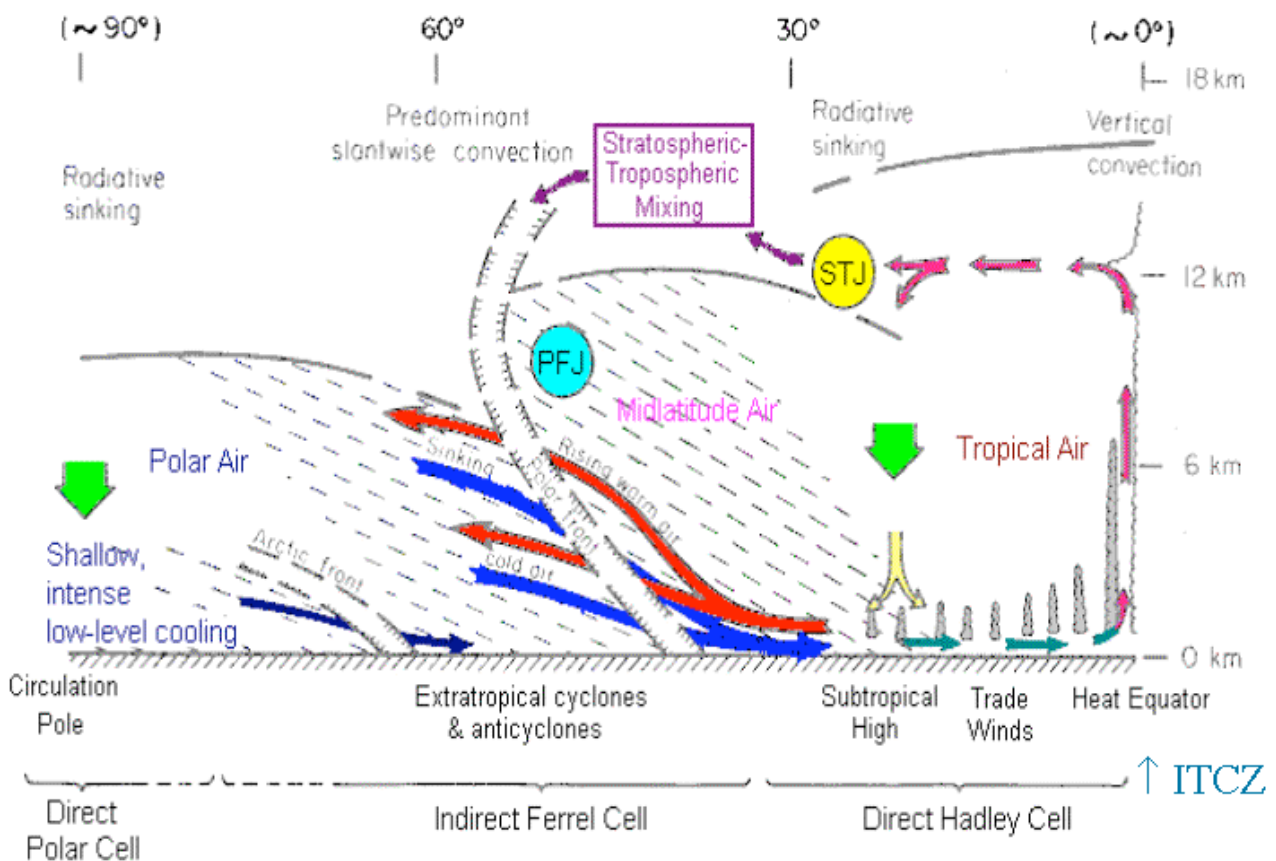


Figure 8 Main convection belts from pole to Equator

In fig. 8, going with the trade winds towards the ITCZ the trade wind cumulus eventually develops into large deep convection towers that reach into the troposphere / stratosphere inversion. Then the air spreads out and cools by radiation into space, until it is cold enough to sink in the descending branch of the Hadley cell and reaches sea level again at about 20° latitude.

We see that the system between -20° and +20° latitude is much simpler and easier to describe than that at higher latitudes, because at low latitude there is no [anti]cyclonic behavior, there are no fronts, no Jet streams. Deep convection pushes up the tropopause to 16 km, i.e. the height that follows from local lapse rate and sea level humidity.

### Conclusion: CO<sub>2</sub> dependence of tropical pacific cooling

The intenser the tropical convective cooling, the colder the air in the upper troposphere becomes. A higher level to which heat is convected increases strongly the ease of radiation into space. Both lapse rate and SST are contained, or regulated, by this ITCZ convective heat transfer. The deep convective heat transfer system maintains itself by a positive feedback, because a stronger radiative cooling of the upper troposphere increases the lapse rate and therefore the convection height. It is a nevertheless a stable system because stronger convection increase heat transfer and lowers the SST, that has an apparent bound at 30 °C.

Higher SST increases heat transfer. This increase in cooling results from:

- 1] the convective height increases due to the rise in specific humidity at sea level,
- 2] the mass transfer driving force [1-rH] at the surface increases,
- 3] wind speed increases also; all trade wind is driven by this ITCZ deep convection.



This results in about 20 W/m<sup>2</sup> flux increase per K SST increase. This is a "negative feedback" so large that the "climate sensitivity" of doubled CO<sub>2</sub> becomes very small as a result. ***The 20 W/m<sup>2</sup>K has to be compared to the 3.7 W/m<sup>2</sup> radiation “forcing” by a doubling of CO<sub>2</sub>. That results in a “climate sensitivity” of 3.7W/m<sup>2</sup> / 20 W/m<sup>2</sup>K =0.2 °C.***

This is very different from what we are told by the climate models, that show a “climate sensitivity” of at least 1.5 °C and at most 6 °C at 2 x CO<sub>2</sub>.

What is wrong here?

### Real world - Model discrepancies

There is a large discrepancy between the observed upper tropospheric temperatures [negative trend] and the temperatures expected by climate models that start from the greenhouse warming hypothesis [positive trend]. Greenhouse models expect as a consequence of the 35% rise in CO<sub>2</sub> that the temperature rise in the tropical troposphere, for example during the 1979-2009 warming period, is much larger [0.3 K/10y] than the 0.15 K/10y surface warming trend. Let us first look to the measured trends as a function of height and latitude: From the official Hadley Center web page <http://www.climatedata.info/Forcing/Forcing/radiosonde.html> we take the following graph:

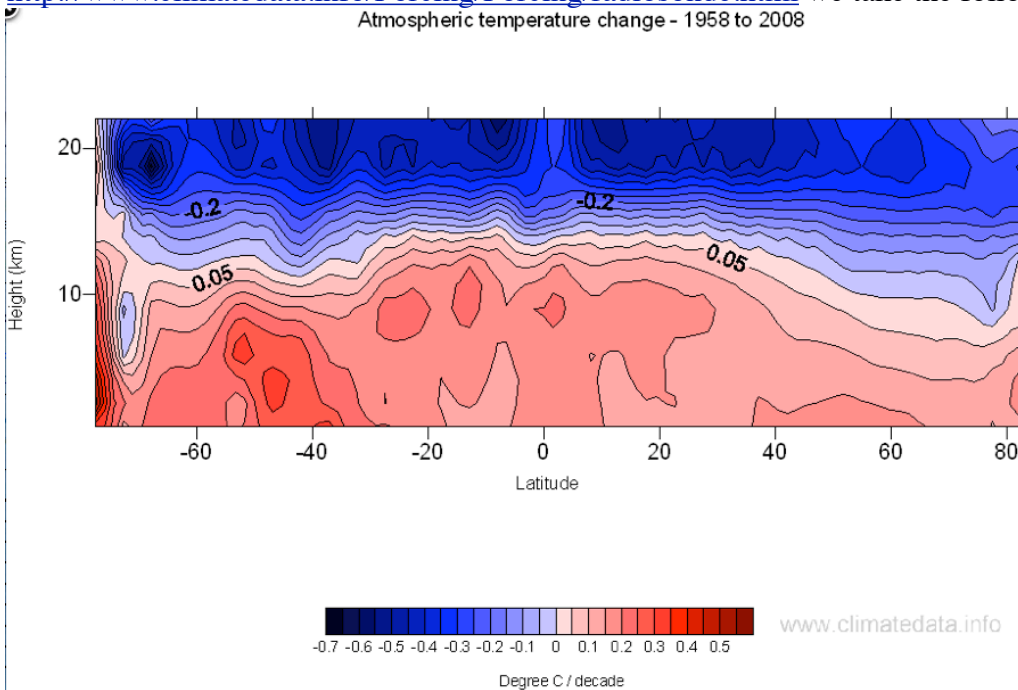


Figure 9 Radiosonde measured trends in atmospheric temperature 1958 - 2008.

Fig. 9 shows that the anomaly in the tropics is indeed a good measure for the global anomaly, not only at the surface, but also up to 20 km in height. Above ca. 12 km there is a cooling trend, which is at 15 km the same as the warming trend at the surface, and at higher altitudes even 5 times as large [-.7 K/10y] as the surface trend. Clearly the rising CO<sub>2</sub> concentration, which is larger than the water concentration at these heights, is the cause of this strong cooling trend. Not much is published of this strong cooling trend due to CO<sub>2</sub>. It is the only effect on temperature of increased CO<sub>2</sub> that can be clearly measured, however.

Another quite unexpected behavior of the higher atmospheric temperature is the reaction to large volcanic eruptions, From <http://hadobs.metoffice.com/hadat/images.html> . The data sources are indicated in the figure itself:

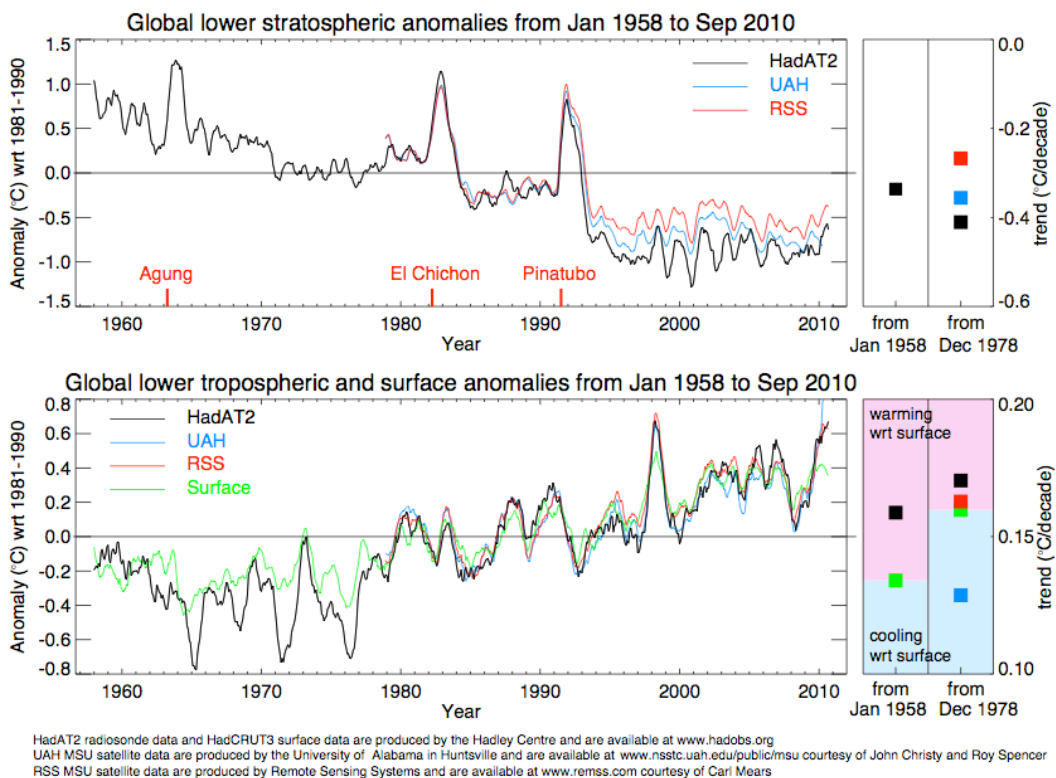


Figure 10. Stratospheric and lower tropospheric temperature trends 1958 - 2010.

We see in fig. 10 that as a trend, the surface warms and the upper atmosphere cools. After a large volcanic eruption, the upper atmospheric temperature increases a full °C. This reaction is much more clear than the surface temperature response. Clearly the volcanic aerosols that are brought far in the stratosphere have a life time over there much longer than in the troposphere, where they rain out. They absorb solar radiation, and heat the atmosphere. This solar radiation does not reach the surface. This brings a cooling of the SST and therefore of the global climate, about a year later.

From AIRS satellite measurements we learn that convection means cooling near the convection column top, 100 hPa in this case, brought about by strong radiative cooling, see fig 11:  
*Observations of convective cooling in the tropical tropopause layer in AIRS data, H. Kim and A. E. Dessler, Atmos. Chem. Phys. Discuss., 4, 7615–7629, 2004* : For each AIRS temperature profile, they looked within ±3 h of the profile measurement time and determine the time history of convection in the 1°x1° box around the measurement. Stage 1: No convection in the previous 3 h, convection starts in the next 3 h, Stage 2: Convection started in the previous 3 h and continues for the next 3 h, Stage 3: On-going convection for the entire 6-h period, Stage 4: Convection on-going during previous 3 h, convection stops in the next 3 h, Stage 5: Convection stopped in the previous 3 h, no convection in the next 3 h. We clearly see that during deep convection locally the 400 kPa level becomes 2 °C warmer and the 100 hPa level or the tropical tropopause level, becomes 2 °C colder. The SST becomes 0.5 to 1 °C colder.

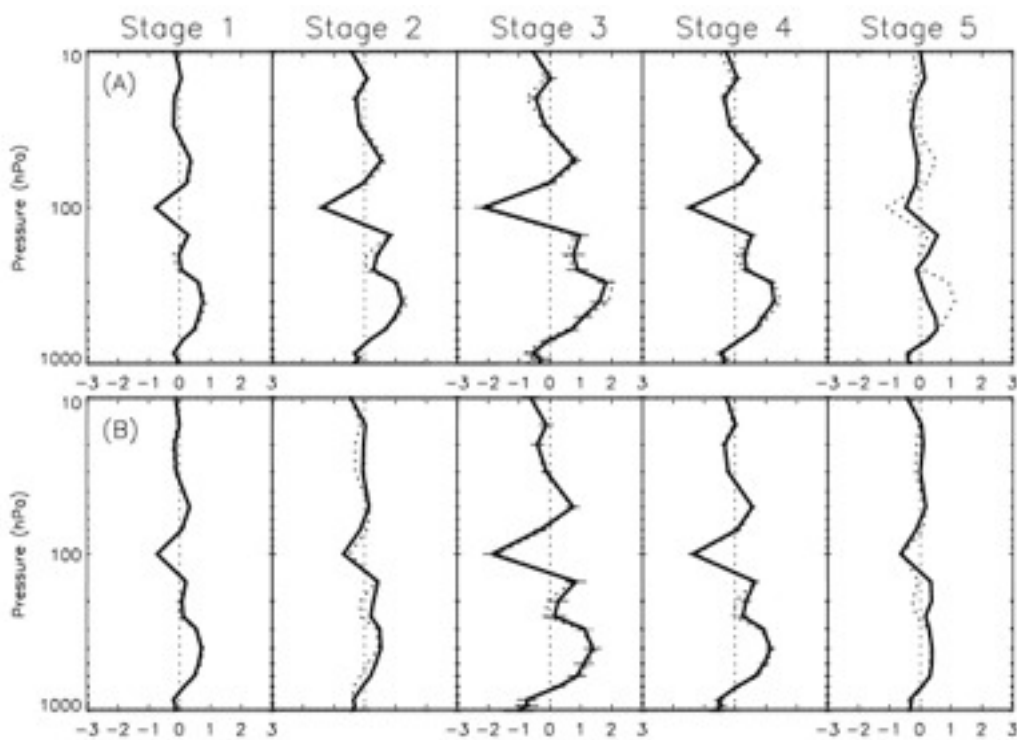


Figure 11 Mean temperature anomaly over convective stages for a) February 2003 and b) July 2003. Dotted lines indicate values from nighttime only. Horizontal bars at each pressure level mean the 95% confidence interval for the mean of the temperature anomaly.

### Warming & cooling trends in different recent periods.

Let us see how these trends differ during warming periods and during longer periods; again from Hadley center sources: [http://hadobs.metoffice.com/hadat/images/update\\_images/zonal\\_trends.png](http://hadobs.metoffice.com/hadat/images/update_images/zonal_trends.png)

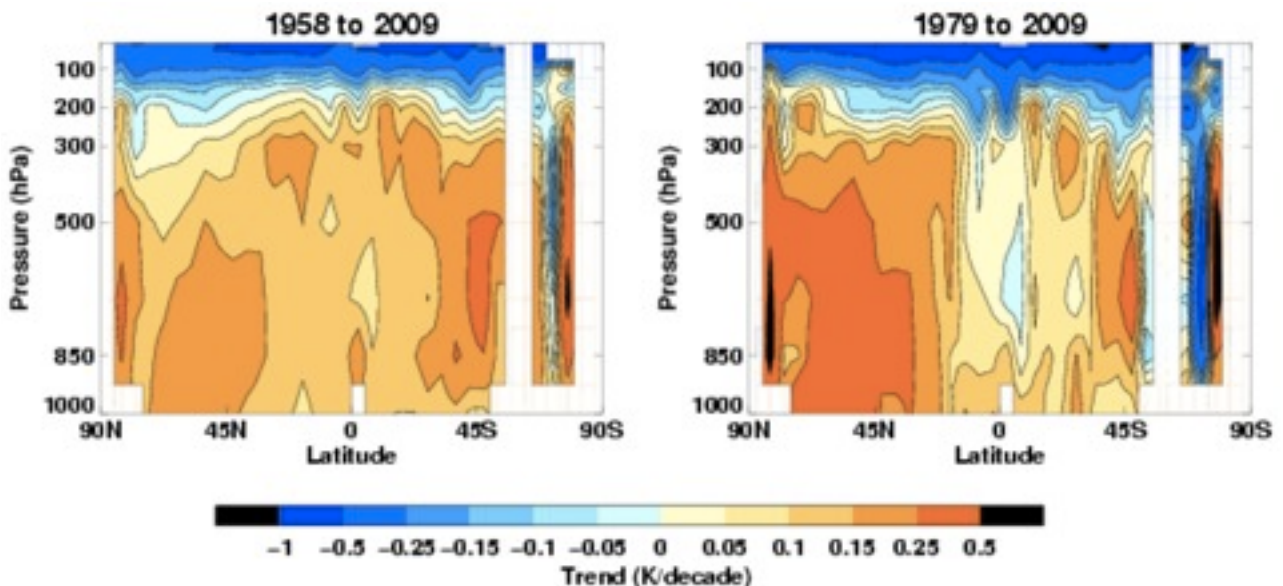


Figure 12 Atmospheric temperature trends as a function of latitude and altitude

The global warming started in 1976 with the “big climate shift”, the trend stopped in 1999 but the climate stayed warm until 2010. We see that in the warming period 1979-2009 not only the warming trend at the surface is higher than in the longer period, but the cooling trend in the high

tropical troposphere is also clearly enhanced. We see even a cooling trend 1979-2009 replacing a warming trend 1958-2009 at the tropical 500-800 hPa height just at the ITCZ.

[http://hadobs.metoffice.com/hadat/images/update\\_images/large\\_area.png](http://hadobs.metoffice.com/hadat/images/update_images/large_area.png)

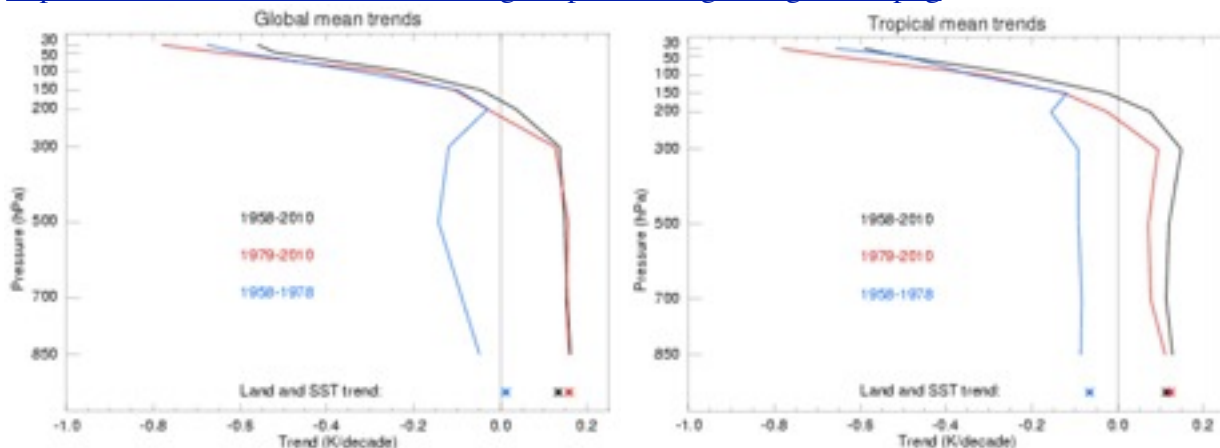


Figure 13 Global and tropical atmospheric temperature trends as a function of altitude

In the two images of fig. 13 we see that the warming occurs mainly after 1979, and the warming up to 300 hPa is not more than on the surface. Above 200 hPa a strong cooling trend is visible. This behavior has been a problem for many, as it falsifies a main point of the global-warming-by-greenhouse-gases- hypothesis. The warming by increased CO<sub>2</sub> can only result from “increased back radiation” from the atmosphere to the surface, and for this the warming of the troposphere due to increased CO<sub>2</sub> must be more than the surface warming. all models predict much more warming at 300 - 400 hPa compared to the surface warming trend. This is not observed.

There has been a large activity to bring models and observations in line, strangely only **by adjusting the measurements instead of adjusting the models**. The radiosonde measurements are adjusted so that they show the larger warming trend around 300 hPa that the models must assume to exist to get antropogenic CO<sub>2</sub> induced warming, or to attribute the surface warming to increased CO<sub>2</sub>. Scores of publications and discussions try to prove this “atmospheric hot spot” must exist in the real world because the models say so. One example I show below:

From: *Toward Elimination of the Warm Bias in Historic Radiosonde Temperature Records—Some New Results from a Comprehensive Intercomparison of Upper-Air Data*, HAIMBERGER et al, *JOURNAL OF CLIMATE*, VOLUME 21, 4587) we take the following figure:

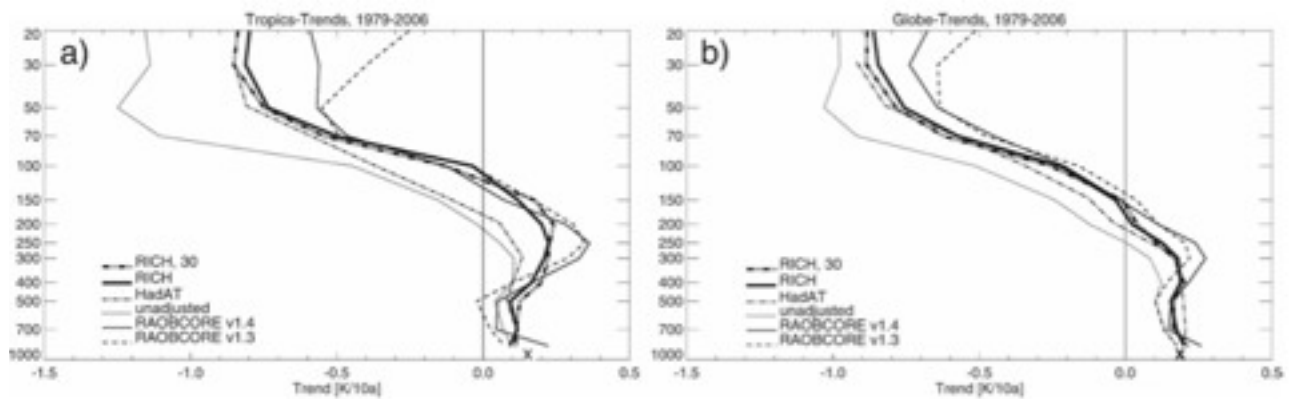


Figure 14 Vertical temperature trend profiles a) for the tropics [20°S-20°N] and b) for the global mean. Thick solid is standard RICH estimate using eight reference stations. Thick dashed-double dotted curve is RICH estimate using 30 reference stations. Thin solid curve is RAOBCORE version 1.4 estimate, thin dashed curve is RAOBCORE version 1.3, and **dotted is from unadjusted radiosonde data**. HadAT2 profiles [thin dashed-dotted] are estimated from less available radiosondes and are indicated for reference. Corresponding surface temperature trends from HadCRUT version 3.0 are denoted with x symbols.

Fig. 14 shows that the *unadjusted* 1979-2006 tropical temperature profile trends in the tropics, left graph, dotted line, shows a constant 0.1 K/decade warming with height until 200 Pa [11 km in the tropics], and above this height a substantial cooling trend, with a minimum of -1.2 K/decade [minus twelve times the surface warming trend!] at 70 Pa. Exactly like the fig.12 observations from Hadoffice show. This behavior does not agree with the accepted theory of Greenhouse-gas induced global warming, that assumes a **decrease** of the convection activity with rising SST, because the temperature and moisture at 500-100 hPa in theory both rise, and this rising  $\theta_e$  prevents convection. This is known as the “hot spot”. It is the main “*positive feedback*” assumed by the models to get the high climate sensitivity to be able to attribute the warming 1976-2010 to the CO<sub>2</sub> increase. It is also called the “super Greenhouse Effect”. It exists only in climate models. This is the reason that so many corrections or adjustments have been proposed to the radiosonde measurements; the maximum adjustment [see left graph] reaching 0.9 K/10y, or 10°C/decade from 1979 to 2009, that makes an adjustment of 2.7 °C between the HadAT temperature measurement and the unadjusted radiosonde measurement. Radiosonde sensors have a precision of 0.1 °C! Physically it is impossible that convection decreases as the driving force for convection increases. Riehl & Malkus measured and quantified this deep convection in 1958 for the first time by flying into thunderstorms and derived the  $\theta_e$  mathematics, which are soundly and simply founded in atmospheric thermodynamics. Thunderstorms are very local phenomena, they cannot and are not well parameterized in climate models. Clearly frequency and intensity of these storms is increasing fast with SST. Any CO<sub>2</sub> in the atmosphere, if it would increase SST, is regulated back by this deep convective cooling mechanism.

**The main error in the climate models is that they suppose heating and moistening, and thus higher  $\theta_e$ , of the upper troposphere by CO<sub>2</sub>, in contradiction with radiosonde and satellite measurements. This assumed heating & moistening leads the model to assume an increase of  $\theta_e$  at this height, which makes deep convection *decrease* as a result of increasing SST, very unphysical as we have seen here above.**

In the real world however, the upper troposphere will dry out as a result of stronger deep convection, because cloud top temperature goes down and condensation efficiency increases with deep convection intensity. In the region that the air spreads from the ITCZ and subsides, radiation into space is therefore enhanced. The lowest temperatures in the troposphere are to be found in the deep convection cumulonimbus tops, sometimes -80 °C. All water is then in solid form, which coalesces easier and snows [rains] out more efficiently. This drying out has been documented well

in the ERA and in the NCEP reanalysis historical time series. But it is hotly contested by IPCC-quoted authors, again because it is incompatible with climate models.

Another discrepancy is the large underestimation of precipitation trends by the models: In the global warming period from 1979 to 2008, we see that the precipitation in the ascending branch of the Hadley cycle increases, that means that the tropical thunderstorms increase in number & strength, and the precipitation in the descending branch decreases, that means that the air in this branch becomes drier, because the deep convection condensation ends at a higher and thus colder level in the atmosphere.

From: Current changes in tropical precipitation Richard P Allan, Brian J Soden, Viju O John, William Ingram and Peter Good, Environ. Res. Lett. 5 (2010) 025205 we take fig 15:

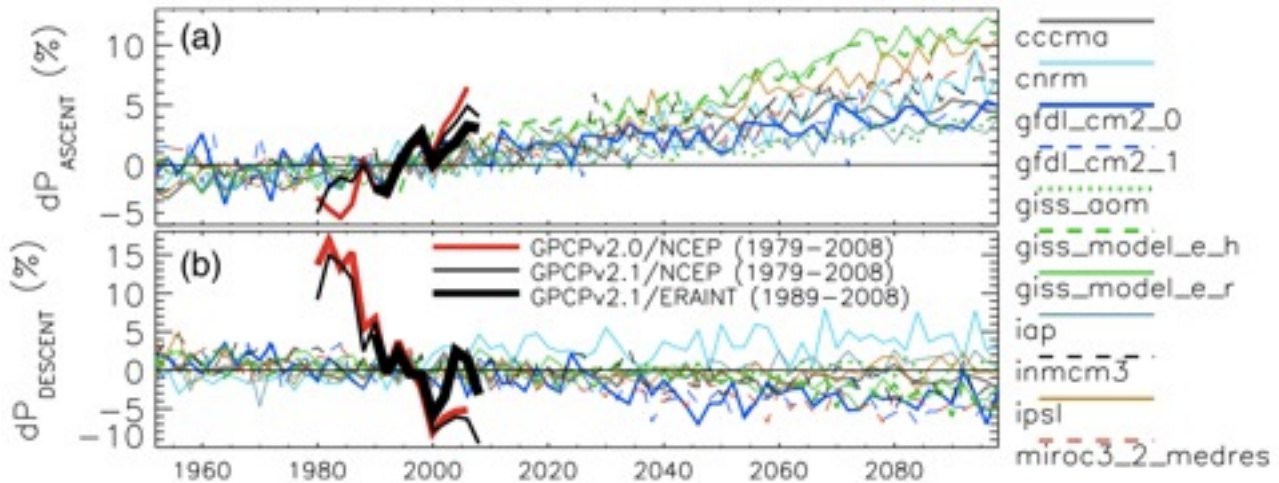


Figure 15 Precipitation anomalies [2-year averages] over a) ascending and b) descending branches of the tropical circulation for CMIP3 models and versions 2.0 and 2.1 GPCP observations applying NCEP or ERA Interim reanalysis vertical motion fields. Updated from Allen & Soden [2007]

All 11 climate models underestimate strongly the observed precipitation anomaly trends, both in the ascending mode [factor 3 underestimation of a rising trend] as in the descending mode [factor 5 underestimation of a lowering trend]. The models just cannot [or do not want to] follow the increase of the hydrological cycle. If they would do that correctly, the resulting climate sensitivity would be much lower. It looks as if the models are made on purpose so, that the resulting climate sensitivity is alarmingly high. It looks as if the observations are adjusted, when they do not fit the models.

Resuming we have three climate stabilizing processes when SST rises: **1]** heat take-up from the ocean rises with  $40 \text{ W/m}^2\text{K}$ , **2]** convection height rises with  $1.5 \text{ km/K}$  SST, and **3]** the spreading air from the ITCZ to the trade wind belt will contain less water enhancing OLR from the lower latitudes.

All these effects are physically well founded. All are clearly measured by numerous independent sources. All point to a large  $20 \text{ W/m}^2$  increase of heat transfer between SST and space for every  $^\circ\text{C}$  SST warming.

### Alternative causes for the global warming

Now we have to find the real cause for the global warming between 1976 and 1998. When it cannot be the  $\text{CO}_2$  increase, it must have another cause. This cause must lie in the tropical Pacific, and indeed it does. [http://www7320.nrlssc.navy.mil/global\\_ncom/animations/eqp/sst12m.gif](http://www7320.nrlssc.navy.mil/global_ncom/animations/eqp/sst12m.gif) gives an animation of the tropical Pacific SST as a function of time December 2009-December 2010:

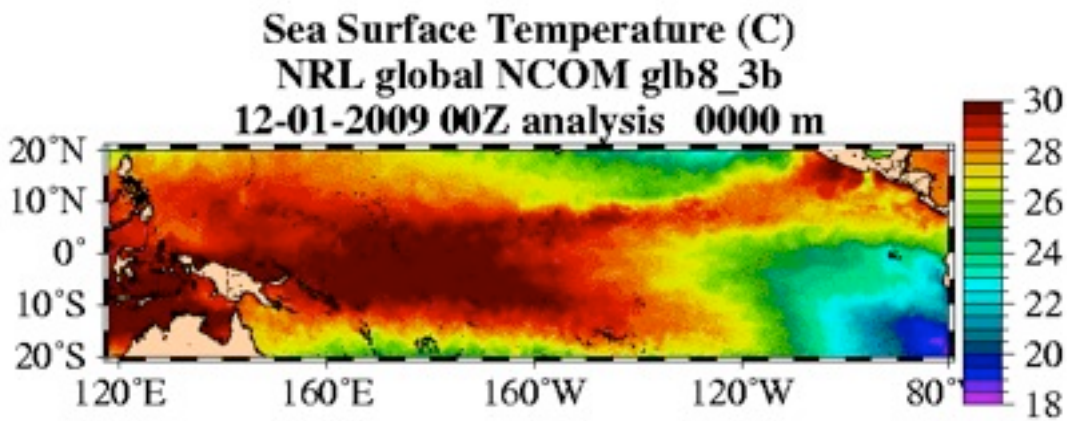


Figure 16 Sea surface temperature animation over the past 12 months. Please click on the link to see the animation, it is very instructive indeed!

Running the animation in fig. 16 we see a large variability. From December 2009 until April 2010, we see a high temperature [El Niño] along most of the region, only at the Southeast corner of the region we see lower temperatures. In April the sea is the warmest. Then in May 2010 we see the beginning of a cold tongue of deep upwelling cold water [La Niña] growing from East to West, reaching almost as far as 160°E longitude in November 2010. The difference or range in SST is large: from 30 °C maximal to 18 °C minimal. The geographic extension of the effect is also very large, about a million square kilometers. We see also a very fast change, in a few days, in this time frame seen as a flickering of SST between 30 and 28 °C in the warm regions. Here one sees the mechanism of cooling: As soon as rising SST reaches a certain value, deep convection sets in and in a matter of hours or days the temperature is brought back a few °C. In the cold tongue, nothing of this kind can be seen. The “thermostat” works only above 27 °C. Only then the convection that starts becomes deep enough.

This large variation in SST with sometimes a duration of many years, large as well in geographic as in SST dimension, is called ENSO or El Niño Southern Oscillation. It has a major influence on the global temperature as we see in fig. 17 the following ENSO and SST history:

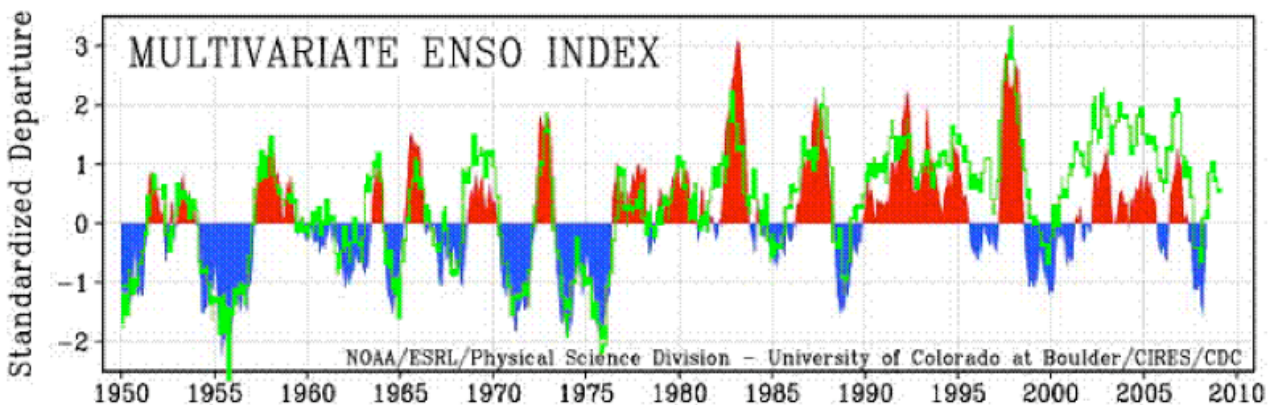


Figure 17 The ENSO index history from 1950 to 2010. The green curve, tropical Pacific SST anomaly, is the same as the red curve in the fig. 1. The red positive and blue negative excursions are the standardized ENSO index or SOI values as a function of time.

Fig. 17 shows that the tropical Pacific SST closely follows the ENSO index. In the period of global warming, the red El Niño events were more frequent than the blue La Niña events, the latter being upwelling of deep cold water before the coast of Peru. **We see that the period of global warming between 1976 and 1999 is simply a period with frequent positive excursions of the ENSO index.** The period 1950 - 1976, with many blue excursions, was one of falling global temperature.

In 1976 the “big climate shift”, the change to frequent red warm excursions. After 1999 there was no global warming anymore, but it stayed warm. CO<sub>2</sub> in the atmosphere rises steadily however during these three different periods. The correlation is clearly with ocean currents, not with CO<sub>2</sub>.

## Galactic Cosmic Rays

For explaining the larger and longer-duration climate excursions, such as the Little Ice Age, or real ice ages for that matter, ENSO-like oscillations will not suffice.

Another, this time external, variable in our climate is the variability in hard Galactic Cosmic Rays [GCR], originating from Galactic supernovae, that are more or less screened off by Solar magnetic fields. GCR, together with very low concentrations of sulphuric acid that are always present, increase the number of cloud condensation nuclei. Most cosmic rays come from the sun, but their energy is in the order of MeV, and therefore they cannot penetrate down to the height where cloud nucleation is important. GCR with energies >13 GeV penetrate down to surface level, leaving thousands of ionized air molecules in their tracks. Variable cloud condensation of course has an immediate effect on temperature, through condensation and rain-out efficiency, through cloud life time [Albrecht effect], cloud whiteness [Twomey effect], cloud cover and resulting absorbed solar radiation.

Henrik Svensmark, Torsten Bondo, and Jacob Svensmark, GEOPHYSICAL RESEARCH LETTERS, 36, 2009 published the following five graphs in fig. 18, data from five different satellites measuring aerosols, cloud water content, liquid water cloud fraction and low infrared sensed cloud cover fraction, just at the time of a Forbush [red broken curve] event:

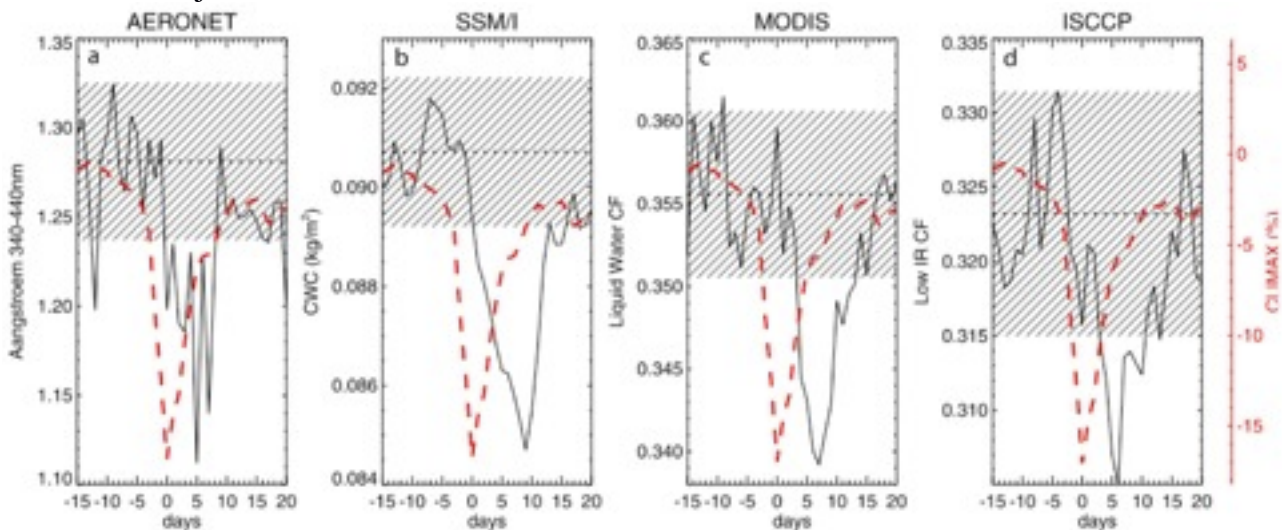


Figure 18 The evolution of [b] cloud water content [SSM/I], [c] liquid water cloud fraction [MODIS], and [d] low IR-detected clouds [ISCCP] is here averaged for the five strongest Forbush decreases that their data sets have in common and is compared with [a] the corresponding evolution of fine aerosol particles in the lower atmosphere [AERONET]. In [a] each data point is the daily mean from about 40 AERONET stations world-wide, using stations with more than 20 measurements a day. Red curves show % changes in GCR neutron counts at Climax. The broken horizontal lines denote the mean for the first 15 days before the Forbush minimum, and the hatched zones show  $\pm 1\sigma$  for the data, estimated from the average variance of a large number of randomly chosen periods of 36 days of each of the four data sets. The effects on clouds and aerosols are not dominated by any single event among the 5 averaged.

A Forbush event is a sudden decrease in Galactic Cosmic Rays [GCR] due to a large plasma outbreak from the Solar Corona. GCR are protons and He nuclei with 10...30 GeV energy, and therefore they can penetrate our atmosphere all the way to the surface, creating large showers of charged atmospheric molecules on their way, <sup>10</sup>Be and <sup>14</sup>C isotopes by spallation from <sup>14</sup>N and



$^{16}\text{O}$  air atoms, as well as neutrons that can be counted with Earth-based instruments. We see, about 5 to 10 days after a sudden 17% decrease of the GCR, that the aerosol concentration decreases with 12.5% after 5 days, the global cloud water content decreases with 6.5% after 9 days, the liquid water cloud fraction decreases with 4.5% after 7 days and the low IR sensed cloud fraction decreases with 5.6% after 6 days.

The mechanism is currently a subject for study at CERN, Genève. First results, see CERN-SPSC-2010-013 SPSC-SR-061, April 7, 2010, from CERN's "CLOUD" experiment confirm the hypothesis: Charged particles from GCR are instrumental in transforming very small but ubiquitous 30 nm  $\text{H}_2\text{SO}_4$  particles into 100 nm cloud condensation nuclei. During a period of high Solar magnetic activity, Sun spots are more frequent, GCR intensity is less and cloud condensation nuclei are less frequent. Clouds then have larger droplets, are less white or reflective, the condensation efficiency increases, the clouds rain out easier, the cloud cover decreases, and the Earth's albedo decreases and as a result the amount of sunlight absorbed at the surface increases. All these trends have been clearly measured during the warming period. These causes global warming; a 1% cloud cover decrease raises the global temperature with 0.5 °C.

In the graph here under, from: Influence of Cosmic Rays on Earth's Climate

Henrik Svensmark\*, PHYSICAL REVIEW LETTERS, VOLUME 81, NUMBER 22 we see that the period of global warming, 1976-1998, is also a period of less GCR intensity:

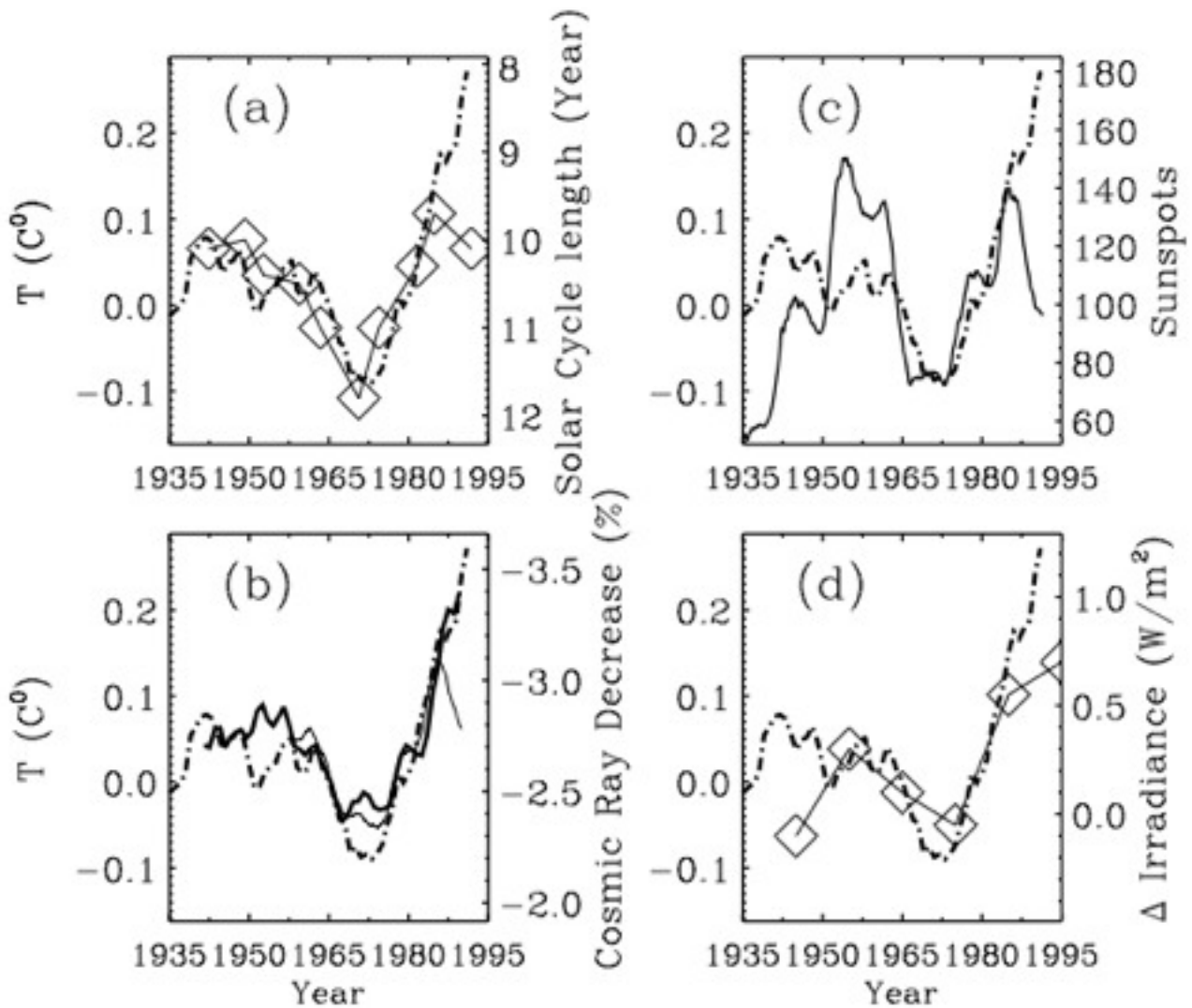


Figure 19 11 year average of northern hemispheric marine and land temperatures (dash-dotted line) compared with (a) unfiltered solar cycle length; (b) 11 year average of cosmic ray flux (from ion chambers 1937 – 1994, normalized to 1965), thick solid line; the thin solid line is cosmic ray flux from Climax, Colorado neutron monitor (arbitrarily scale); (c) 11 year average of relative

sunspot number; (d) decade variation in reconstructed solar irradiance (zero level corresponds to  $1367 \text{ W/m}^2$ , adapted from Lean et al. [6]). Note the 11 year average has removed the solar cycle in (b) and (c).

Clearly the global temperature anomaly correlates in fig. 19 with GCR level and solar cycle length, and [much] less with Solar irradiance and the number of sunspots.

The warming [until 1950] cooling [1950-1976] warming again [1976-1995] correlate much stronger with GCR intensity than with  $\text{CO}_2$  in the atmosphere, the latter being monotonically rising.

*COSMIC RAYS, PARTICLE FORMATION, NATURAL VARIABILITY OF GLOBAL CLOUDINESS, AND CLIMATE IMPLICATIONS* Fangqun Yu, Atmospheric Sciences Research Center, State University of New York, Albany, New York, USA gives us the following three graphs:

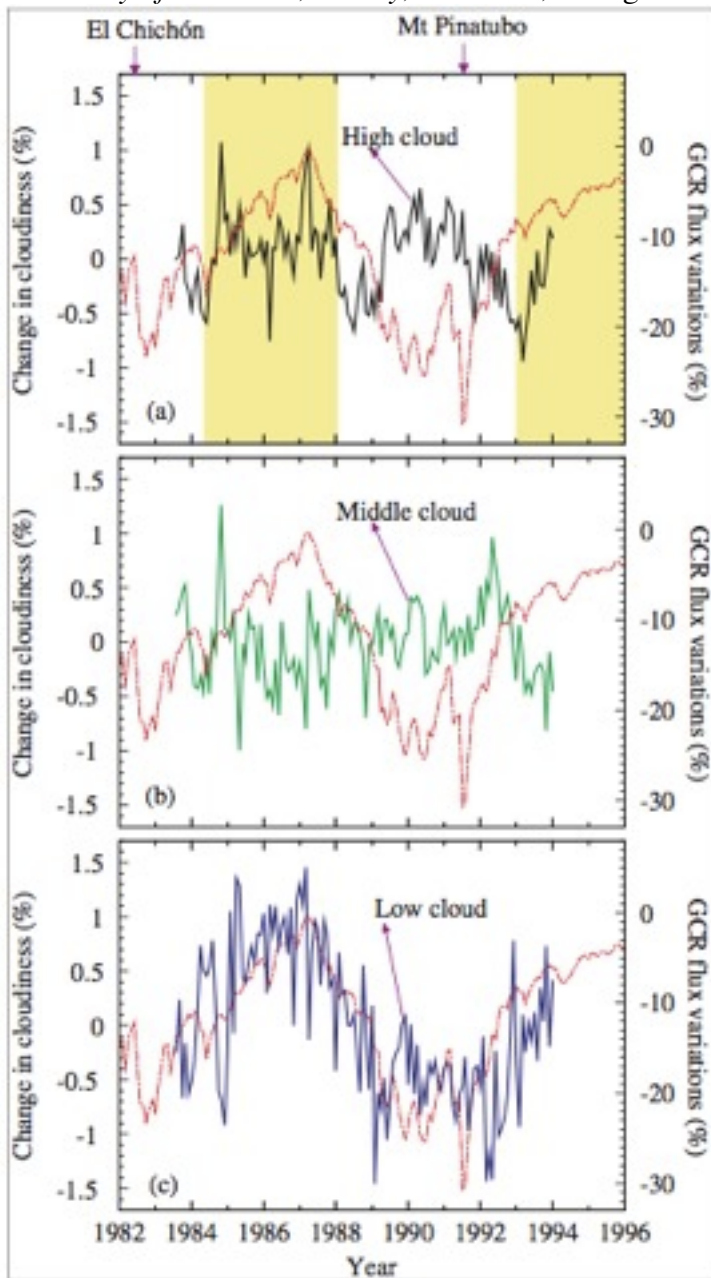


Figure 20 The global average monthly mean anomalies of (a) high, (b) middle, and (c) low IR cloud cover during last solar cycle. The variations of galactic cosmic ray (GCR) fluxes as measured from CLIMAX (normalized to May, 1965) are also indicated in each panel (dot-dashed lines). The

shaded areas in Figure 2(a) corresponding to the years that global high cloudiness might have been affected by volcano eruptions and El Niño event.

We see from fig. 20 that only the low clouds, which have a cooling effect on the climate, are correlated with GCR, not the middle and the high clouds. Indeed, the period with decreasing low clouds, 1986-1992, is one of rising temperatures. Cloud condensation nuclei due to ionizing radiation are abundant in the higher atmosphere, because lower energetic solar protons can penetrate to this height. Only GCR of energies of >13 GeV penetrate as far as the surface. The correlation with climate is not without hiatus however, but it is in any case better than the correlation with CO<sub>2</sub>.

*Manley G (1974) Central England temperatures: Monthly means 1659–1973. Q J R Met Soc 100:389–405 gives central England temperatures, <sup>10</sup>Be as an indicator of solar variability and climate, J. Beer et al, Swiss Federal Institute for Environmental Science and Technology (EAWAG), compare with <sup>10</sup>Be values.*

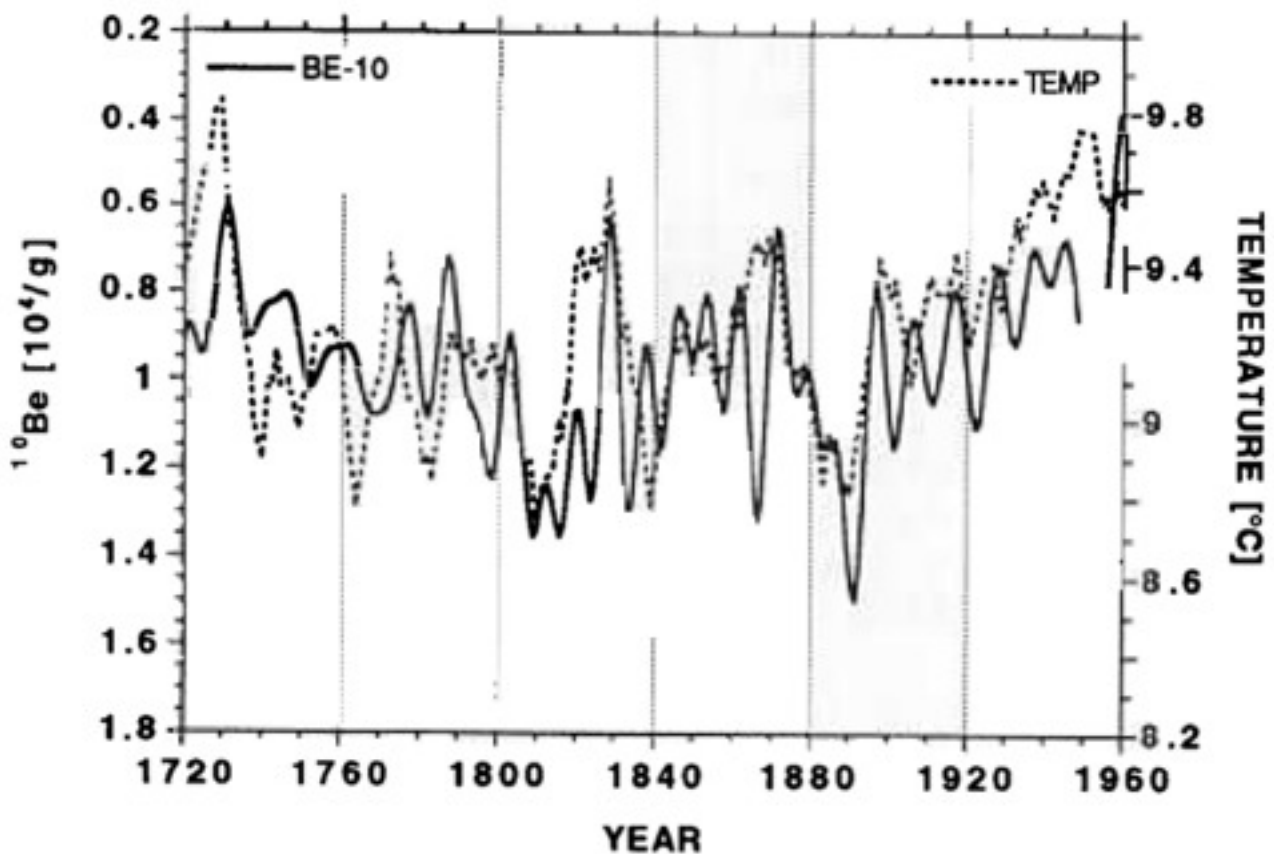


Figure 21 Comparison of the low-pass filtered <sup>10</sup>Be data from Dye 3 with the temperature record from central England [Manley 1974]

Fig. 21 shows a clear correlation of temperature with GCR intensity, for which the <sup>10</sup>Be isotope in well-dated sediments is witness, and cold periods. Note the inverted scale for <sup>10</sup>Be. Dye3 is a Greenland ice core. Central England is our oldest instrumental temperature record. More <sup>10</sup>Be, stronger GCR, more cloud condensation nuclei, more and whiter clouds, higher albedo, lower temperature.

One might ask why the Greenland GCR should correlate with Central England temperatures, but we have to realize that the GCR intensity has a solar-system-wide extension, so that all local temperatures on earth should equally feel the impact.

There is no possibility that the CO<sub>2</sub> amount in the atmosphere would be the cause of these climate changes from 1720 until 1960: it has known no period of decreasing.

Before the age of temperature measurement we have to resort to other variables that are a measure of climate, such as grain prices that rise after cold and bad growing seasons: We see a persistent correlation of <sup>10</sup>Be and grain prices in fig. 22. High <sup>10</sup>Be means strong GCR's, more and whiter clouds, lower sunshine, lower temperatures, shorter growing seasons, and higher grain prices:

**INFLUENCE OF SOLAR ACTIVITY ON STATE OF WHEAT MARKET IN MEDIEVAL ENGLAND, Lev A. Pustilnik, Gregory Yom Din. They conclude:**

- a) The clear coincidence between the statistical properties of the distributions of intervals between wheat price bursts in medieval England (1259-1702) and intervals between minima of solar cycles (1700-2000);
- b) The existence of 100% sign correlation between high wheat prices and states of minimal solar activity established on the basis of <sup>10</sup>Be data for Greenland ice measurements for the period 1600-1700.

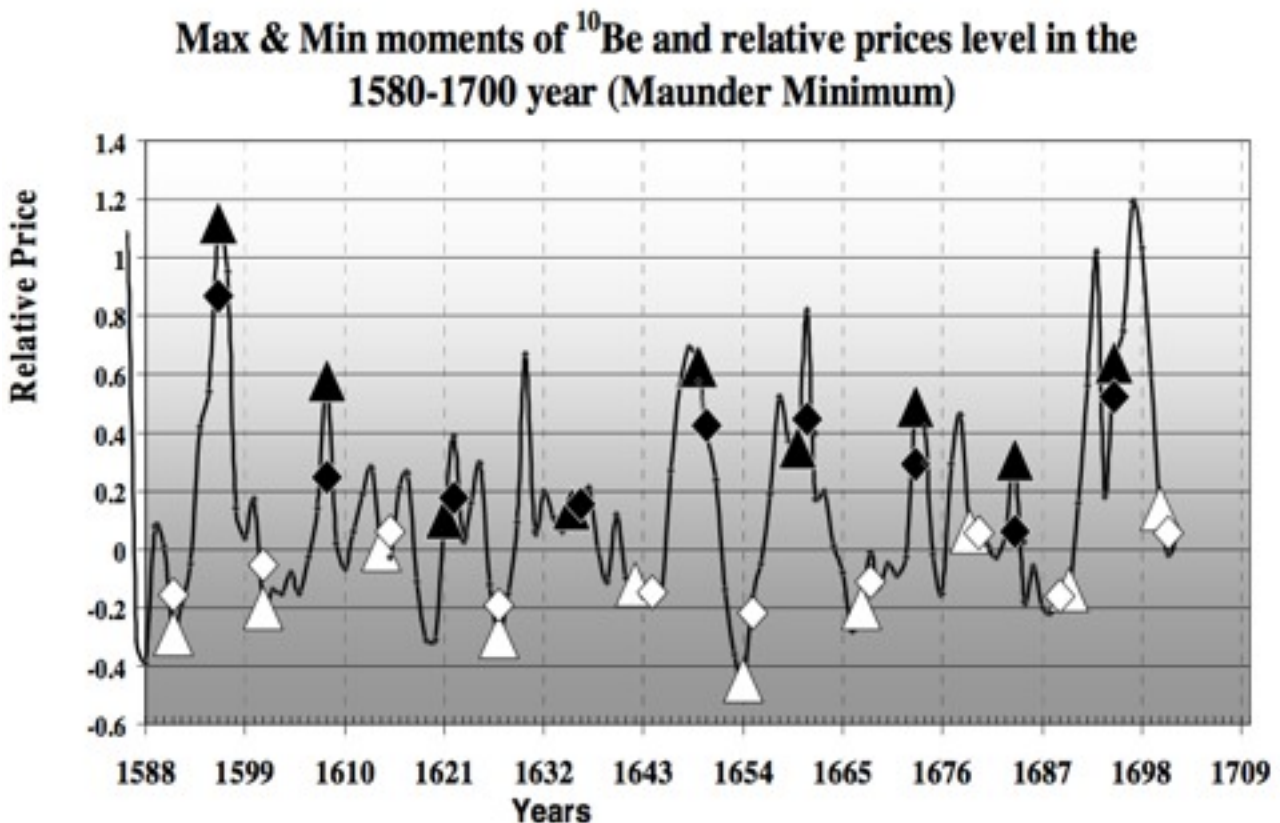


Figure 22 Consistent differences in prices at moments of maximum and minimum states of solar activity (1600-1700). White and black rectangles are prices averaged for 3-years intervals centered on moments of maximum and minimum of solar activity, white and black triangles are prices in the moment of the maximum and minimum.

The recovery from the penultimate ice age [termination II] begins tens of thousands of years **before** the peak in the June insolation of the Milanković cycle. This has been known a long time as "the causation problem" and has been a mystery until the <sup>10</sup>Be deposition rate had been correlated with the temperature proxies:

CERN-PH-EP/2004-027, 18 June 2004, THE GLACIAL CYCLES AND COSMIC RAYS, J. Kirkby, A. Mangini, R.A. Muller; give the following set of time histories:

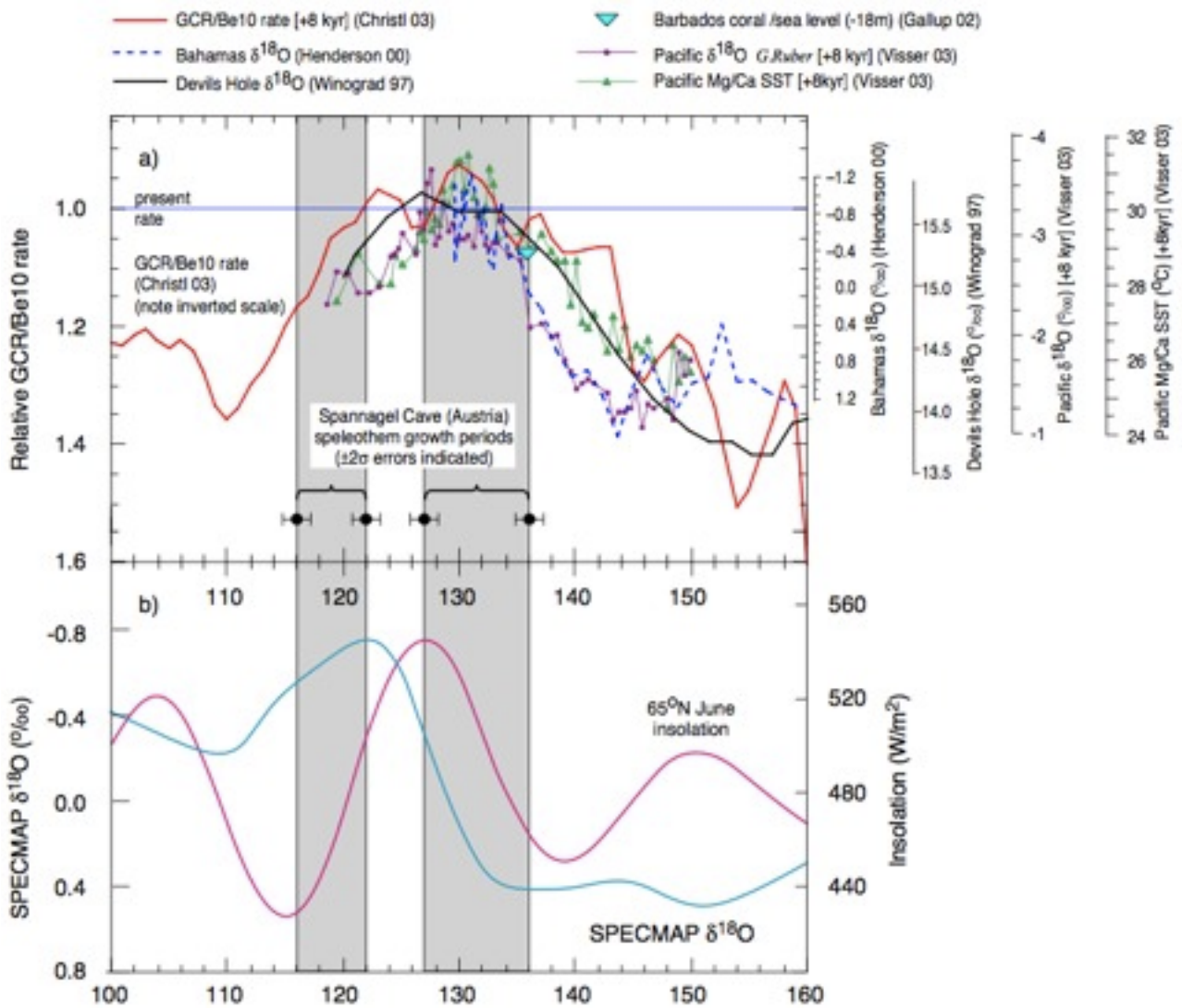


Figure 23 Timing of glacial Termination II, 130 ky ago. a) The GCR rate together with the Bahamian  $\delta_{18}\text{O}$  record, the date when the Barbados sea level was within 18 m of its present value, the  $\delta_{18}\text{O}$  temperature record from Devils Hole cave, Nevada, and the Visser *et al.* measurements of the Indo-Pacific Ocean surface temperature and  $\delta_{18}\text{O}$  records. The GCR rate and the Visser *et al.* data are shifted earlier by 8 kyr in order to correct for estimated systematic errors in the SPECMAP timescale, on which they are based. The growth periods of stalagmite SPA 52 from Spannagel Cave, Austria, are indicated by grey bands and black points. b) The 65°N June insolation and the SPECMAP  $\delta_{18}\text{O}$  record.

It is clear from fig. 23 that a steady decrease, mind the inverted scale of 10Be [GCR rate], from 1.5 to 0.9 times the current rate over a period of 30000 years, has been the driver for termination II, not the 65° June insolation, which comes 8000 years later, and not the world's temperature rise as seen in the specmap, which comes 12000 years later. In the same paper we find also an explication of the ice-house - hothouse climate states that interchange every 140 million years. This is the period of the solar system being in a star-dense spiral arm; more GCR, colder, ice-house; and just between two galactic arms, less GCR, warmer, hothouse climate state.

**Conclusion**

Our present climate is due to an increased length of the last interglacial period, more than 10000 years, due to a low level of GCR that maintains a low cloud cover, a low albedo, more absorbed sunshine and a pleasant climate. In the very long run, we need not mind about CO<sub>2</sub> or global warming, but instead about lower GCR activity and global cooling. There is no way we can influence GCR activity. It originates in active black holes and imploding supernovae in the Milky Way, modulated by weaker or stronger solar and interplanetary magnetic fields that screen off the GCR particles.